Journal of Molecular Structure 1051 (2013) 265–270

Contents lists available at ScienceDirect

Journal of Molecular Structure

journal homepage: www.elsevier.com/locate/molstruc

Assessment of the molecular structure of natrodufrénite – $NaFe^{2+}Fe_5^{3+}(PO_4)_4(OH)_6 \cdot 2(H_2O)$, a secondary pegmatite phosphate mineral from Minas Gerais, Brazil

Andrés López [a], Ray L. Frost [a,*], Yunfei Xi [a], Ricardo Scholz [b], Fernanda Maria Belotti [c], Érika Ribeiro [b]

[a] Discipline of Nanotechnology and Molecular Science, Science and Engineering Faculty, Queensland University of Technology, GPO Box 2434, Brisbane, Queensland 4001, Australia
[b] Geology Department, School of Mines, Federal University of Ouro Preto, Campus Morro do Cruzeiro, Ouro Preto, MG 35,400-00, Brazil
[c] Federal University of Itajubá, Campus Itabira, Itabira, MG 35,903-087, Brazil

HIGHLIGHTS

- We have studied the mineral natrodufrénite using SEM-EDX and vibrational spectroscopy.
- The chemical formula was determined.
- Raman bands of natrodufrénite were measured.
- The molecular structure was assessed.

ARTICLE INFO

Article history:
Received 26 March 2013
Accepted 12 August 2013
Available online 19 August 2013

Keywords:
Natrodufrénite
Phosphate
Pegmatite
Infrared spectroscopy
Raman spectroscopy

ABSTRACT

The mineral natrodufrénite a secondary pegmatite phosphate mineral from Minas Gerais, Brazil, has been studied by a combination of scanning electron microscopy and vibrational spectroscopic techniques. Electron probe analysis shows the formula of the studied mineral as $(Na_{0.88}Ca_{0.12})_{\sum 1.00}(Fe^{2+}_{0.72}Mn_{0.11}Mg_{0.08}Ca_{0.04}Zr_{0.01}Cu_{0.01})_{\sum 0.97}(Fe^{3+}_{4.89}Al_{0.02})_{\sum 4.91}(PO_4)_{3.96}(OH_{6.15}F_{0.07})_{6.22} \cdot 2.05(H_2O)$. Raman spectroscopy identifies an intense peak at 1003 cm^{-1} assigned to the PO_4^{3-} ν_1 symmetric stretching mode. Raman bands are observed at 1059 and 1118 cm^{-1} and are attributed to the PO_4^{3-} ν_3 antisymmetric stretching vibrations. A comparison is made with the spectral data of other hydrate hydroxy phosphate minerals including cyrilovite and wardite. Raman bands at 560, 582, 619 and 668 cm^{-1} are assigned to the ν_4 PO_4^{3-} bending modes and Raman bands at 425, 444, 477 and 507 cm^{-1} are due to the ν_2 PO_4^{3-} bending modes. Raman bands in the 2600–3800 cm^{-1} spectral range are attributed to water and OH stretching vibrations. Vibrational spectroscopy enables aspects of the molecular structure of natrodufrénite to be assessed.

1. Introduction

Natrodufrénite is hydrated hydroxyl basic iron and sodium phosphate mineral and shows general chemical formula expressed by $NaFe^{2+}Fe_5^{3+}(PO_4)_4(OH)_6 \cdot 2(H_2O)$. The mineral was first described from Pluherlin Castle, Brittany, France [1]. Natrodufrénite is a member of the dufrénite group that also includes burangaite, matioliite, dufrénite and gayite [2]. Natrodufrénite usually occurs as secondary phosphate mineral in phosphorus bearing pegmatites with primary triplite and zwieselite [2,3].

Granitic pegmatites are important sources for industrial minerals, gemstones and rare minerals for the collectors market. The diversity of minerals is the result of chemical evolution due to the superposition of different process, including the magmatic, methasomatic, hydrothermalism and weathering. A complete characterization of the mineral assemblage can be an important tool in the study of the geological evolution of such rocks [4]. In some phosphate rich pegmatites the mineral assemblage can include more than 60 minerals [5–7]. In recent years, the application of spectroscopic techniques to understand the structure of phosphates is increasing, with special attention to pegmatite phosphates, especially due to being a non destructive technique (RAMAN) or by using small amounts of sample (infrared).

Farmer [8] divided the vibrational spectra of phosphates according to the presence, or absence of water and/or hydroxyl units in the minerals. In aqueous systems, Raman spectra of phosphate oxyanions show a symmetric stretching mode (ν_1) at 938 cm^{-1}, the antisymmetric stretching mode (ν_3) at 1017 cm^{-1}, the symmetric bending mode (ν_2) at 420 cm^{-1} and the ν_4 mode at 567 cm^{-1} [9–12]. The value for the ν_1 symmetric stretching vibration of PO_4 units as determined by infrared spectroscopy

* Corresponding author. Tel.: +61 7 3138 2407; fax: +61 7 3138 1804.
E-mail address: r.frost@qut.edu.au (R.L. Frost).

0022-2860/$ - see front matter © 2013 Elsevier B.V. All rights reserved.
http://dx.doi.org/10.1016/j.molstruc.2013.08.018

was given as 930 cm^{-1} (augelite), 940 cm^{-1} (wavellite), 970 cm^{-1} (rockbridgeite), 995 cm^{-1} (dufrénite) and 965 cm^{-1} (beraunite). The position of the symmetric stretching vibration is mineral dependent and a function of the cation and crystal structure. The fact that the symmetric stretching mode is observed in the infrared spectrum affirms a reduction in symmetry of the PO_4 units.

The value for the ν_2 symmetric bending vibration of PO_4 units as determined by infrared spectroscopy was given as 438 cm^{-1} (augelite), 452 cm^{-1} (wavellite), 440 and 415 cm^{-1} (rockbridgeite), 455, 435 and 415 cm^{-1} (dufrénite) and 470 and 450 cm^{-1} (beraunite). The observation of multiple bending modes provides an indication of symmetry reduction of the PO_4 units. This symmetry reduction is also observed through the ν_3 antisymmetric stretching vibrations. Augelite shows infrared bands at 1205, 1155, 1079 and 1015 cm^{-1} [13,14]; wavellite at 1145, 1102, 1062 and 1025 cm^{-1}; rockbridgeite at 1145, 1060 and 1030 cm^{-1}; dufrénite at 1135, 1070 and 1032 cm^{-1}; and beraunite at 1150, 1100, 1076 and 1035 cm^{-1}.

In this work, spectroscopic investigation of a monomineral natrodufrénite sample from Divino das Laranjeiras, Minas Gerais, Brazil has been carried out. The analysis includes spectroscopic characterization of the structure with infrared and Raman spectroscopy.

2. Methods

2.1. Sample preparation

An olive green aggregate of natrodufrénite was obtained from the collection of the Geology Department of the Federal University of Ouro Preto, Minas Gerais, Brazil, with sample code SAB-009. The sample is from a granitic pegmatite located in Divino das Laranjeiras, eastern Minas Gerais. Natrodufrénite forms a botryoidal aggregate up to 3 cm in association with hydroxylherderite and ushkovite. The sample was gently crushed in an agate mortar and the pure fragments were hand selected under a stereomicroscope Leica MZ4. One fragment was prepared in polyester resin for quantitative chemical analysis. The polishing was undertaken in the sequence of 9 μm, 6 μm and 1 μm diamond paste MetaDI® II Diamond Paste – Buhler, using water as a lubricant, with a semi-automatic MiniMet® 1000 Grinder–Polisher–Buehler.

2.2. Scanning electron microscopy (SEM)

Natrodufrénite samples were coated with a thin layer of evaporated carbon. Secondary electron and backscattering images were obtained using a JEOL-JSM840A scanning electron microscope from the Physics Department of the Federal University of Minas Gerais, Belo Horizonte. Qualitative chemical analyses by SEM in the EDS mode were produced to support the mineral characterization and determine the concentration of the elements by Electron probe micro-analysis.

2.3. Electron micro probe (EMP)

EPMA was carried in a selection of two single crystals, with the performance of five spots per crystal. The chemical analysis was carried out with a Jeol JXA8900R spectrometer from the Physics Department of the Federal University of Minas Gerais, Belo Horizonte. For each selected element was used the following standards: Fe – Magnetite, Mg – MgO, Mn – Rodhonite, P – $Ca_2P_2O_7$, Ca – Anorthite100, Na – Albite100, Al – Anorthite100, K – Microcline, Zr – Badelleyite, Sr – Celestite, Pb – Galena, Ba – Barite, Cu – CuS and F – Fluorite. The epoxy embedded natrodufrénite sample was coated with a thin layer of evaporated carbon. The electron probe microanalysis in the WDS (wavelength dispersive spectrometer) mode was obtained at 15 kV accelerating voltage and beam current of 10 nA.

2.4. Raman microprobe spectroscopy

Crystals of natrodufrénite were placed on a polished metal surface on the stage of an Olympus BHSM microscope, which is equipped with 10×, 20×, and 50× objectives. The microscope is part of a Renishaw 1000 Raman microscope system, which also includes a monochromator, a filter system and a CCD detector (1024 pixels). The Raman spectra were excited by a Spectra-Physics model 127 He–Ne laser producing highly polarised light at 633 nm and collected at a nominal resolution of 2 cm^{-1} and a precision of ±1 cm^{-1} in the range between 200 and 4000 cm^{-1}. Repeated acquisitions on the crystals using the highest magnification (50×) were accumulated to improve the signal to noise ratio of the spectra. The spectra were collected over night. Raman Spectra were calibrated using the 520.5 cm^{-1} line of a silicon wafer. The Raman spectrum of at least 10 crystals was collected to ensure the consistency of the spectra.

2.5. Infrared spectroscopy

Infrared spectra were obtained using a Nicolet Nexus 870 FTIR spectrometer with a smart endurance single bounce diamond ATR cell. Spectra over the 4000–525 cm^{-1} range were obtained by the co-addition of 128 scans with a resolution of 4 cm^{-1} and a mirror velocity of 0.6329 cm/s. Spectra were co-added to improve the signal to noise ratio. The infrared spectra are given in the supplementary information.

Spectral manipulation such as baseline correction/adjustment and smoothing were performed using the Spectracalc software package GRAMS (Galactic Industries Corporation, NH, USA). Band component analysis was undertaken using the Jandel 'Peakfit' software package that enabled the type of fitting function to be selected and allows specific parameters to be fixed or varied accordingly. Band fitting was done using a Lorentzian–Gaussian cross-product function with the minimum number of component bands used for the fitting process. The Gaussian–Lorentzian ratio was maintained at values greater than 0.7 and fitting was undertaken until reproducible results were obtained with squared correlations of r^2 greater than 0.995.

3. Results and discussion

3.1. Chemical characterization

The BSI images of a natrodufrénite crystal aggregate studied in this work are shown in Fig. 1. The quantitative chemical analysis of natrodufrénite is presented in Table 1. The water content was calculated by stoichiometry. The chemical composition indicates an intermediate member of the natrodufrénite–dufrénite series with predominance of the natrodufrénite in relation to dufrénite end-member. The results also show variable amounts of Ba that due to the ionic ratio was considered in substitution to Na. and Ca, which partially replaces Mg and Na, respectively.

$$(Na_{0.88}Ca_{0.12})_{\Sigma 1.00}(Fe^{2+}_{0.72}Mn_{0.11}Mg_{0.08}Ca_{0.04}Zr_{0.01}Cu_{0.01})_{\Sigma 0.97}$$
$$(Fe^{3+}_{4.89}Al_{0.02})_{\Sigma 4.91}(PO_4)_{3.96}(OH_{6.15}F_{0.07})_{6.22}\cdot 2.05(H_2O)$$

3.2. Vibrational spectroscopy

The Raman spectrum of natrodufrénite over the 100–4000 cm^{-1} spectral range is provided in Fig. 2a. This spectrum displays the Ra-

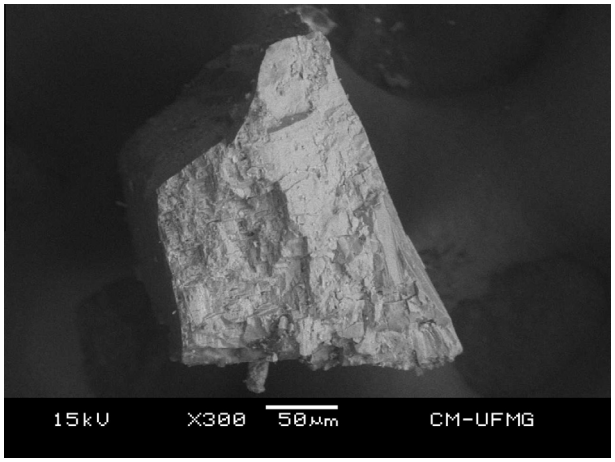

Fig. 1. Backscattered electron image (BSI) of a natrodufrénite fragment up to 0.5 mm in length.

man bands, their position and relative intensities. It is noted that there are large parts of the spectrum where no intensity is observed. Therefore, the spectrum is subdivided into sections where significant intensity is observed, based upon the type of vibration being studied. The infrared spectrum of natrodufrénite is displayed in Fig. 2b. This figure shows the position and relative intensities of the infrared bands. There are large spectral regions where no intensity is observed; therefore, the spectrum is subdivided into sections depending upon the types of vibration being examined. There has been very little published on the Raman spectrum of dufrénite. There is a spectrum of natrodufrénite given on the RRUFF data base at http://rruff.info/dufrenite/display=default/. This Raman spectrum is shown in Supplemenatry information. However no assignment or description of the bands is given. Also the spectral region of the hydroxyl stretching region is not shown. Such bands are important for the determination of the molecular structure of the mineral. Some infrared spectra of dufrénite may be found in some data bases but the data is not readily accessible.

The Raman spectrum of natrodufrénite over the 800–1400 cm^{-1} spectral range is shown in Fig. 3a. The spectrum is dominated by an intense somewhat broad peak at 1003 cm^{-1} assigned to the PO_4^{3-} ν_1 symmetric stretching mode. Two Raman bands are observed at 1059 and 1118 cm^{-1} and are attributed to the PO_4^{3-} ν_3 antisymmetric stretching vibrations. The Raman spectrum of a natrodufrénite from the RRUFF data base is given in Supplementary information. This spectrum shows an intense band at 995 cm^{-1} with a high wavenumber shoulder at 995 cm^{-1}. These bands may be assigned to the PO_4^{3-} ν_1 symmetric stretching mode This RRUFF spectrum also shows three bands at 1053, 1162 and 1186 cm^{-1}. These bands may be assigned to the PO_4^{3-} ν_3 antisymmetric stretching vibrations. The Raman bands are broad. This suggests that each peak may be composed of a number of overlapping bands. It is interesting to compare the spectra of natrodufrénite

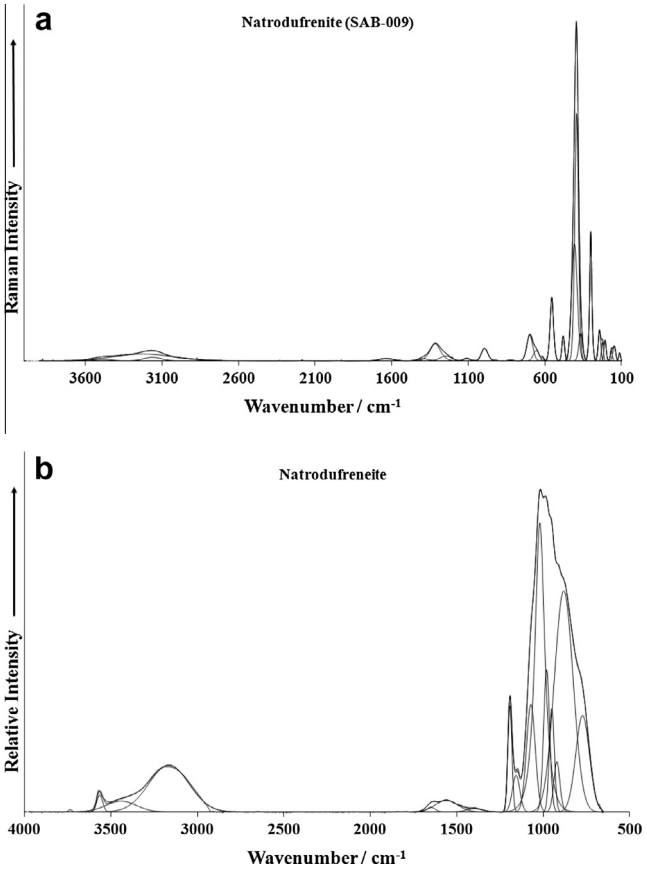

Fig. 2. (a) Raman spectrum of natrodufrénite over the 100–4000 cm^{-1} spectral range. (b) Infrared spectrum of natrodufrénite over the 500–4000 cm^{-1} spectral range.

Table 1
Chemical composition of natrodufrénite from Minas Gerais (mean of eight electron microprobe analyses). H_2O calculated by stoichiometry.

Constituent	wt.%	Range (wt.%)	Number of atoms	Probe standard
P_2O_5	30.94		3.96	$Ca_2P_2O_7$
FeO	5.70		0.72	Magnetite
Fe_2O_3	43.01		4.89	Calculated by stoichiometry
MgO	0.37	0.28–0.45	0.08	MgO
Al_2O_3	0.13	0.07–0.20	0.02	Anorthite100
CaO	0.98	0.85–1.11	0.16	Anorthite100
Na_2O	3.00	2.83–3.09	0.88	Albite100
K_2O	0.02	0.00–0.05	0.00	Microcline
MnO	0.83	0.71–0.98	0.11	Rodhonite
ZrO_2	0.13	0.04–0.21	0.01	Badelleyite
SrO	0.02	0.00–0.04	0.00	Celestite
PbO	0.02	0.00–0.09	0.00	Galena
BaO	0.03	0.00–0.13	0.00	Barite
CuO	0.04	0.00–0.06	0.01	CuS
H_2O	10.16	H_2O	2.05	Calculated by TG
		OH	6.15	
F	0.15	0.11–0.17	0.07	Fluorite
Total	96.64		9.90	

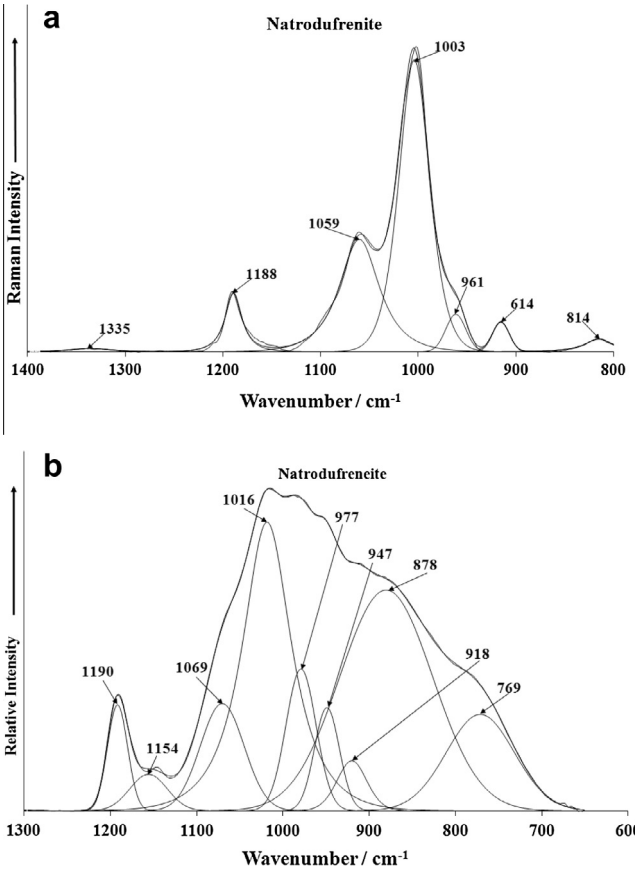

Fig. 3. (a) Raman spectrum of natrodufrénite over the 800–1400 cm^{-1} spectral range. (b) Infrared spectrum of natrodufrénite over the 500–1300 cm^{-1} spectral range.

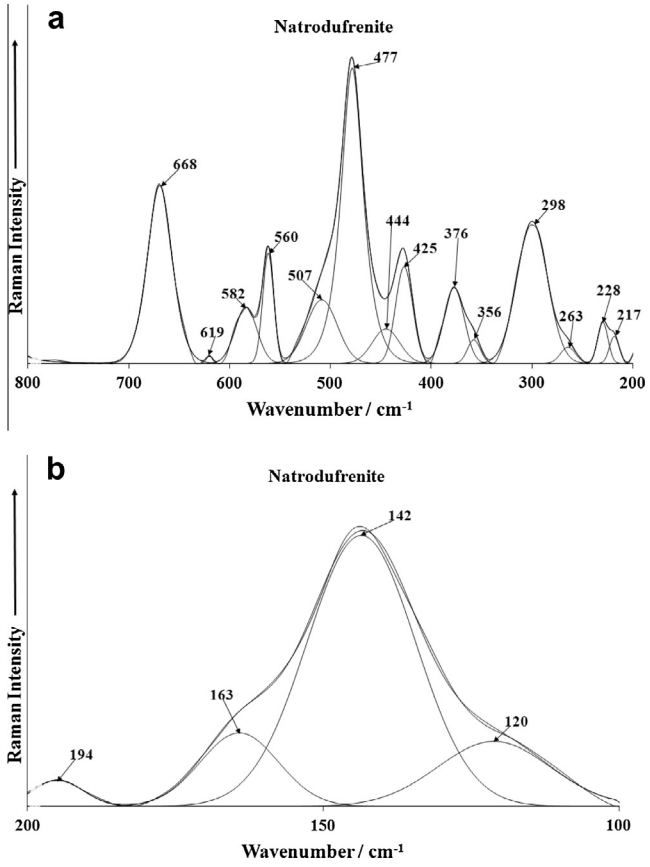

Fig. 4. (a) Raman spectrum of natrodufrénite over the 300–800 cm^{-1} spectral range. (b) Raman spectrum of natrodufrénite over the 100–300 cm^{-1} spectral range.

with other minerals containing sodium and iron, such as cyrilovite $Na(Fe^{3+})_3(PO_4)_2(OH)_4{\cdot}2(H_2O)$. The Raman spectrum of cyrilovite is dominated by two intense bands at 992 and 1055 cm^{-1}. These two bands are assigned to the ν_1 PO_4^{3-} symmetric stretching vibrations. Two intense bands are observed reflecting two non-equivalent phosphate units in the cyrilovite structure. A comparison may be made with the spectrum of wartdite. The Raman spectrum is dominated by two intense bands at around 995 and 1051 cm^{-1}. The spectra appear to differ considerably from that obtained by Breitinger et al. [15]. Breitinger et al. used FT-Raman to obtain their spectrum and found overlapping Raman bands at 999 and 1033 cm^{-1} and assigned these bands to the ν_1 PO_4^{3-} symmetric stretching and ν_3 PO_4^{3-} antisymmetric stretching modes. In the Raman spectrum of cyrilovite, a series of low intensity bands are noted at 1105, 1136, 1177 and 1184 cm^{-1}. These bands are assigned to the ν_3 PO_4^{3-} antisymmetric stretching modes. The Raman spectrum of wardite shows a group of low intensity bands are observed at 1084, 1108, 1120, 1140 and 1186 cm^{-1}. Breitinger et al. [15] did not report any bands in these positions in the Raman spectrum of synthetic wardite.

The complimentary infrared spectrum of natrodufrénite over the 600–1300 cm^{-1} spectral range is illustrated in Fig. 3b. The spectrum shows a broad band with some spectral features. The infrared band at 1016 cm^{-1} may be assigned to the PO_4^{3-} ν_1 symmetric stretching mode. The infrared bands at 1069, 1154 and 1190 cm^{-1} are assigned to the PO_4^{3-} ν_3 antisymmetric stretching vibrations. Other infrared bands as determined by band component analysis are observed at 769, 918, 878, 947 and 977 cm^{-1}. Some of these bands can be attributed to water librational and hydroxyl deformation modes.

The Raman spectrum of natrodufrénite over the 200–800 cm^{-1} spectral range is reported in Fig. 4a and the Raman spectrum of the natrodufrénite in the 100–200 cm^{-1} spectral range is given in Fig. 4b. This spectrum (Fig. 4a) may be subdivided into sections. The first section is the 600–800 cm^{-1} region, the bands around 500 cm^{-1} and the bands between 300 and 400 cm^{-1}. Raman bands at 560, 582, 619 and 668 cm^{-1} are assigned to the ν_4 PO_4^{3-} bending modes. Raman bands are found at 557, 580 and 660 cm^{-1} in the RRUFF spectrum of natrodufrénite, in harmony with the bands found in this work.

The Raman bands at 425, 444, 477 and 507 cm^{-1} are due to the ν_2 PO_4^{3-} bending modes. Raman bands found in the RRUFF spectrum are observed at 422, 475 and 506 cm^{-1}. It is again worthwhile to compare the spectra of natrodufrénite with that of cyrilovite. Raman bands for cyrilovite are observed at 612 and 631 cm^{-1} and are assigned to the ν_4 out of plane bending modes of the PO_4^{3-} and $HOPO_3^{2-}$ units. In the Raman spectrum of wardite, bands are observed at 605 and 618 cm^{-1} with shoulders at 578 and 589 cm^{-1}. Breitinger et al. assigned these bands to $\nu(Al(O/OH)_6)$ stretching vibrations. No phosphate bending modes in the work of Breitinger et al. were reported.

Raman bands at 668 cm^{-1} are assigned to the out-of-plane vibrations of POH units. Farmer [8] tabled this band at 750 cm^{-1}. In the infrared spectrum (Fig. 3b), infrared bands are observed at 769 and 878 cm^{-1}. These bands may be due to the out-of-plane vibrations of POH units. The Raman bands at 298, 356 and 376 cm^{-1} are attributed to metal–oxygen stretching bands. In the RRUFF spectrum, Raman bands are observed at 287 and 367 cm^{-1}. The Raman bands in the 100–200 cm^{-1} spectral range (Fig. 4b) are assigned to lattice vibrations. Prominent bands are ob-

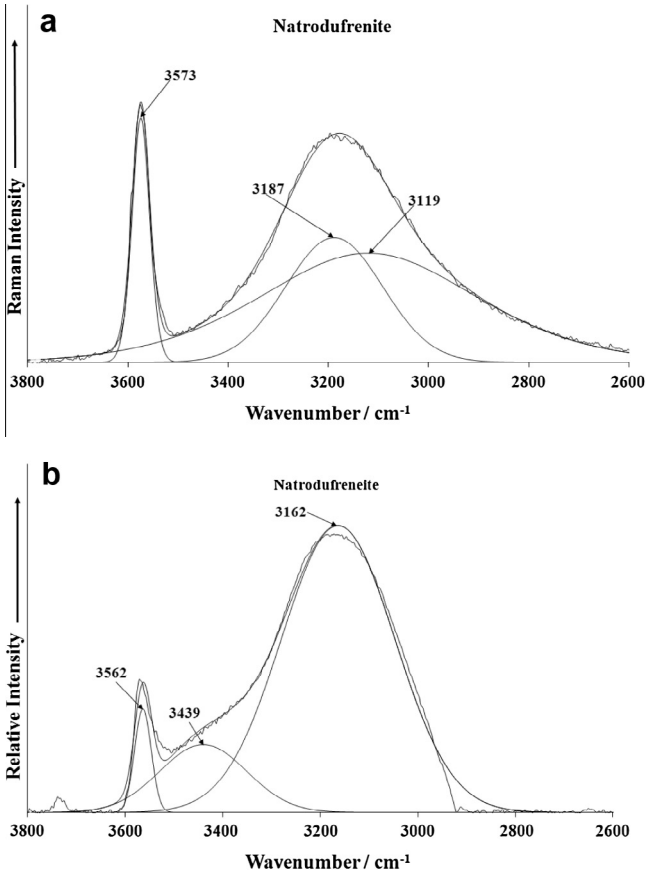

Fig. 5. (a) Raman spectrum of natrodufrénite over the 2600–4000 cm^{-1} spectral range. (b) Infrared spectrum of natrodufrénite over the 2600–4000 cm^{-1} spectral range.

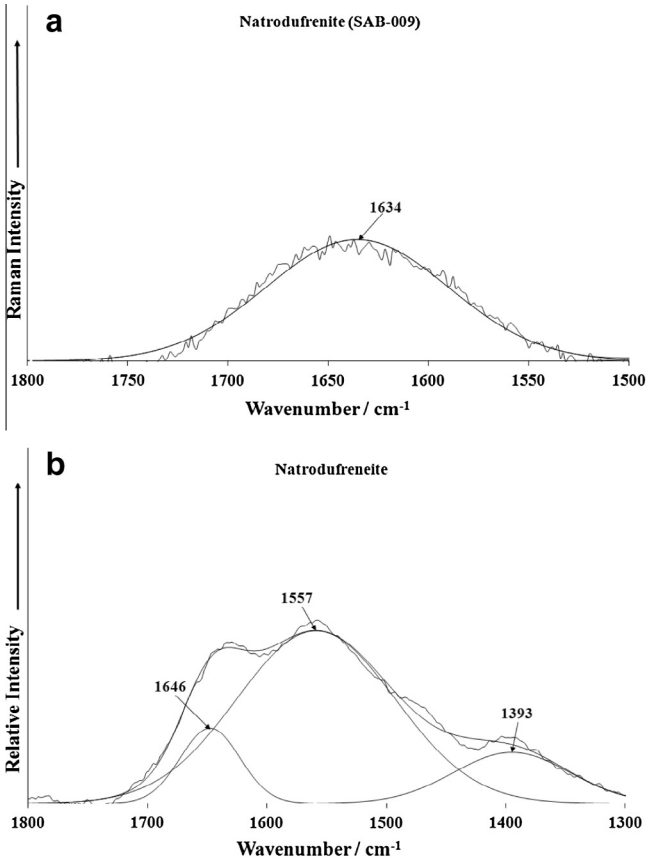

Fig. 6. (a) Raman and (b) Infrared spectrum of natrodufrénite in the 1500–1800 cm^{-1} spectral range.

served at 120, 142 and 163 cm^{-1}. These bands may be simply described as lattice vibrations.

The Raman spectrum of natrodufrénite in the 2600–3800 cm^{-1} spectral range is shown in Fig. 5a. The Raman spectrum is composed of basically two bands at 3187 and 3573 cm^{-1}. This latter band is assigned to the OH stretching vibration. The former band is ascribed to water stretching vibrations. Intense Raman bands for cyrilovite are found at 3328 and 3452 cm^{-1} with a broad shoulder at 3194 cm^{-1} and are assigned to OH stretching vibrations.

The complimentary infrared spectrum is given in Fig. 5b. Two strong bands are observed at 3162 and 3562 cm^{-1}. These bands are in harmony with the bands observed in the Raman spectrum. The latter band is assigned to the stretching vibrations of the hydroxyl units and the former to water stretching vibrations. In the infrared spectrum of cyrilovite sharp infrared bands are observed at 3485 and 3538 cm^{-1}. Broad infrared bands are found at 2893, 3177 and 3311 cm^{-1}. Tarte et al. reported the infrared spectrum of wardite and cyrilovite. They found that O–H stretching frequencies are distributed into 2 spectra regions: 2 very broad bands near 2950 and 3300 cm^{-1}, which are due to H_2O mols. engaged in short H bonds; and 2 very sharp and strong peaks (3550 and 3495 cm^{-1} for pure cyrilovite, 3621 and 3555 cm^{-1} for pure wardite) due to the stretch of hydroxyl group. Sharp infrared bands for wardite are observed at 3544 and 3611 cm^{-1} and are attributed to the OH stretching vibrations of the hydroxyl units. A sharp band in the infrared spectrum is observed at 3480 cm^{-1} for the sample from Utah. This band may be due to FeOH stretching vibrations. Breitinger et al. [15] found infrared bands at 3520 (vw), 3545 (s), 3585 (sh) and 3613 cm^{-1} (m). Breitinger et al. states that the ν(OH) modes in the two independent pairs of symmetry-correlated OH groups classify as 2a + 2b; with the correlation splitting between a and b species depending on the distances in each of the pairs [15]. The ν(OH) region of IR spectra of wardite shows two sharp bands (3613 and 3545 cm^{-1}) with two weak shoulders or satellites (3580 and 3520 cm^{-1}). It is likely that the two sharp infrared bands are due to two independent and non-equivalent OH units.

The Raman spectrum of natrodufrénite in the 1500–1800 cm^{-1} spectral range is reported in Fig. 6a. There appears to be one broad band centered upon 1634 cm^{-1} assigned to the water bending mode. The width of the band is in harmony with the broad bands observed in the OH stretching region. The infrared spectrum in this spectral range is displayed in Fig. 6b. The infrared band at 1646 cm^{-1} is ascribed to the water bending vibration. Raman bands for cyrilovite are observed at 1599 and 1634 cm^{-1}. These bands are assigned to water bending modes. In contrast, the infrared spectrum of cyrilovite shows significant intensity. Water is a very strong infrared absorber. Infrared bands are observed at 1599 and 1650 cm^{-1} and are assigned to water bending modes. Infrared bands for wardite are observed at 1549, 1670 and 1748 cm^{-1}. The bands in this region result from correlation splitting as a result of the short distance and orientation of the H_2O molecules. Additional bands for wardite are observed at 1417 and 1476 cm^{-1}. The assignment of these bands is due to OH deformation modes. The presence or absence of these bands depends upon the Fe/Al ration in the cyrilovite/wardite mineral samples.

4. Conclusions

We have studied the phosphate mineral natrodufrénite, a member of the dufrénite group that also includes burangaite, matioliite, dufrénite and gayite, using a combination of electron microscopy

and vibrational spectroscopy. Natrodufrénite is hydrated hydroxyl basic iron and sodium phosphate mineral of general chemical formula expressed by $NaFe^{2+}Fe^{3+}_5(PO_4)_4(OH)_6 \cdot 2(H_2O)$, and as such lends itself to analysis using vibrational spectroscopic techniques. Electron probe analysis shows the formula to be $(Na_{0.88}Ca_{0.12})_{\sum 1.00}(Fe^{2+}_{0.72}Mn_{0.11}Mg_{0.08}Ca_{0.04}Zr_{0.01}Cu_{0.01})_{\sum 0.97}(Fe^{3+}_{4.89}Al_{0.02})_{\sum 4.91}(PO_4)_{3.96}(OH_{6.15}F_{0.07})_{6.22}\cdot 2.05(H_2O)$.

Vibrational spectroscopy enables the structure of natrodufrénite to be assessed. Raman spectroscopy identifies an intense peak at 1003 cm^{-1} assigned to the PO^{3-}_4 ν_1 symmetric stretching mode. Raman bands are observed at 1059 and 1118 cm^{-1} and are attributed to the PO^{3-}_4 ν_3 antisymmetric stretching vibrations. In the main, the phosphate anion is not distorted in the structure of natrodufrénite. The fact that only symmetric stretching mode is observed means that at least from a spectroscopy point of view, the phosphate units are equivalent in the structure of natrodufrénite. The observation of multiple bands in both the ν_4 and ν_2 PO^{3-}_4 bending spectral range implies some distortion of the phosphate anion.

The Raman spectrum of natrodufrénite in the hydroxyl stretching region is composed of two bands at 3187 and 3573 cm^{-1}, assigned to the water and hydroxyl unit stretching vibration. The peaks are quite broad. This suggests some variation in the hydrogen bond distances between the OH units and the phosphate anion. Certainly, vibrational spectroscopy enables an assessment of the structure of natrodufrenite at the molecular level to be made.

Acknowledgements

The financial and infra-structure support of the Discipline of Nanotechnology and Molecular Science, Science and Engineering Faculty of the Queensland University of Technology, is gratefully acknowledged. The Australian Research Council (ARC) is thanked for funding the instrumentation. R. Scholz thanks to CNPq – Conselho Nacional de Desenvolvimento Científico e Tecnológico (Grant No. 306287/2012-9).

Appendix A. Supplementary material

Supplementary data associated with this article can be found, in the online version, at http://dx.doi.org/10.1016/j.molstruc.2013.08.018.

References

[1] F. Fontan, F. Pillard, F. Permingeat, Bull. Min. 105 (1982) 321–326.
[2] A.R. Kampf, F. Colombo, J.G. del Tanago, Am. Min. 95 (2010) 386–391.
[3] J. Sejkora, R. Skoda, P. Ondrus, P. Beran, C. Susser, J. Czech Geol. Soc. 51 (2006) 103–147.
[4] M. Baijot, F. Hatert, S. Philippo, Can. Min. 50 (2012) 1531–1554.
[5] T.J. Campbell, W.L. Roberts, Min. Rec. 17 (1986) 237–254.
[6] O.V. Knorring, E. Condliffe, Geol. J. 22 (1987) 253–270.
[7] J.P. Cassedanne, A. Baptista, Min. Rec. 30 (1999) 347–365.
[8] V.C. Farmer, Mineralogical Society Monograph 4: The Infrared Spectra of Minerals, Mineralogical Society, London, 1974.
[9] R.L. Frost, T. Kloprogge, P.A. Williams, W. Martens, T.E. Johnson, P. Leverett, Spectrochim. Acta 58A (2002) 2861–2868.
[10] R.L. Frost, W. Martens, P.A. Williams, J.T. Kloprogge, Min. Mag. 66 (2002) 1063–1073.
[11] R.L. Frost, W.N. Martens, T. Kloprogge, P.A. Williams, Neues Jahr. Min. (2002) 481–496.
[12] R.L. Frost, P.A. Williams, W. Martens, J.T. Kloprogge, P. Leverett, J. Raman Spectrosc. 33 (2002) 260–263.
[13] R.L. Frost, Spectrochim. Acta 60A (2004) 1439–1445.
[14] R.L. Frost, M.L. Weier, K.L. Erickson, O. Carmody, S.J. Mills, J. Raman Spectrosc. 35 (2004) 1047–1055.
[15] D.K. Breitinger, H.H. Belz, L. Hajba, V. Komlosi, J. Mink, G. Brehm, D. Colognesi, S.F. Parker, R.G. Schwab, J. Mol. Struct. 706 (2004) 95–99.